The Journal of Experimental Biology 204, 3241–3250 (2001)
Printed in Great Britain © The Company of Biologists Limited 2001
JEB3512

SPREAD OF SYNAPTIC POTENTIALS THROUGH ELECTRICAL SYNAPSES IN RETZIUS NEURONES OF THE LEECH

Francisco F. De-Miguel*, Mariana Vargas-Caballero and Elizabeth García-Pérez
Departamento de Biofísica, Instituto de Fisiología Celular, UNAM, Apartado Postal 70-253, 04510, D.F., México
*e-mail: ffernand@ifisiol.unam.mx

Accepted 6 July 2001

Summary

We studied the spread of excitatory postsynaptic potentials (EPSPs) through electrical synapses in Retzius neurones of the leech *Haementeria officinalis*. The pair of Retzius neurones in each ganglion is coupled by a non-rectifying electrical synapse. Both neurones displayed synchronous EPSPs of varying amplitudes and rise times. The kinetics of synchronous EPSPs was similar in 79 % of the EPSP pairs. In the remaining 21 %, one EPSP was smaller and slower than the other, suggesting its passive spread from the other neurone. The proportion of these events increased to 75 % in the presence of Mg^{2+} in the bathing fluid. This spread of EPSPs from one neurone to another was tested by producing artificial EPSPs by current injection into the soma of one Retzius neurone. The artificial EPSPs were smaller and arrived more slowly at the soma of the coupled neurone. The coupling ratios for the EPSPs were proportional to the coupling ratio for long steady-state pulses in different neuronal pairs. Our results showed that EPSPs spread from one Retzius neurone to the other and support the idea that EPSP spread between electrically coupled neurones may contribute to the integration processes of neurones.

Key words: synapse, electrical synapse, integration, leech, gap junction, *Haementeria officinalis*.

Introduction

Electrical activity patterns in neurones arise from the integration of multiple synaptic inputs acting in concert. The original concept of integration predicts that one neurone summates the excitatory and inhibitory influences converging upon it to produce a new output signal (Fatt, 1957; Coombs et al., 1957; for reviews, see Nicholls et al., 1992; Yuste and Tank, 1996). Diverse mechanisms contribute to the integration process in single neurones, including the production of dendritic spikes (Spencer and Kandel, 1961; Andersen et al., 1966; Llinás and Nicholson, 1971; Llinás and Hess, 1976; Llinás and Sujimori, 1980), the activation of voltage-dependent Na^+ and Ca^{2+} currents (Deisz et al., 1991; Hirsch and Gilbert, 1991; Schwindt and Crill, 1995; Stuart and Sakmann, 1995; Haag and Borst, 1996; Lipowsky et al., 1996; Gillessen and Alzheimer, 1997; Seamans et al., 1997; Margulis and Tang, 1998) and non-linear summation of EPSPs (Wessel et al., 1999).

The fact that many central neurones of adult invertebrates and vertebrates are electrically coupled (Bennett et al., 1963; Auerbach and Bennett, 1969; Baker and Llinás, 1971; Nicholls and Purves, 1972; Korn et al., 1973; Llinás et al., 1974; Schmalbruch and Jahnsen, 1981; Marder and Eisen, 1984; Abbott et al., 1991; McMahon, 1994; Hatton and Yang, 1994; Wolszon et al., 1995; Galarreta and Hestrin, 1999; Gibson et al., 1999) makes it possible that the arrival of synaptic potentials from other neurones will affect the integration process. One clear example is the stomatogastric system of crustaceans, where the spread of inhibitory postsynaptic potentials through electrically coupled neurones contributes to the regulation of the timing of the pyloric rhythm (Marder and Eisen, 1984).

In this paper, we studied the spread of synaptic potentials from one neurone to another in pairs of electrically coupled Retzius neurones in the Mexican leech *Haementeria officinalis*. Each of the 21 segmental ganglia of the leech central nervous system contains a strikingly similar number of neurones distributed in a stereotyped manner (Payton, 1981). Retzius cells are the largest neurones in each ganglion and release most of the serotonin in the animal (Willard, 1981; Henderson, 1983). This modulates behaviour patterns such as swimming (Willard, 1981; Nusbaum and Kristan, 1986; Nusbaum et al., 1987), shortening (Sahley, 1995) and local bending (Kristan, 1982; Lockery and Kristan, 1990). The two Retzius neurones in each segmental ganglion are coupled by a non-rectifying electrical synapse, presumably formed by contacts between the neuropilar branches (Lent, 1973; Smith et al., 1975; Mason and Leake, 1978), and display spontaneous synchronous EPSPs (Hagiwara and Morita, 1962; Eckert, 1963) from which they produce action potentials. In addition, they receive a polysynaptic input from pressure-sensitive neurones (Szczupak and Kristan, 1995). By collecting simultaneous recordings from both Retzius neurones of a pair

under different experimental conditions and producing artificial EPSPs by current injection into one of the neurones, we have shown that EPSPs spread from one Retzius neurone to the other. The possible effects of this spread of EPSPs on integration are discussed.

Materials and methods

Preparation and dissection

Experiments were carried out in isolated ganglia from adult leeches *Haementeria officinalis* at room temperature (20–25 °C). Intersegmental ganglia were dissected out and pinned in Sylgard-coated dishes containing leech Ringer composed of (mmol l^{-1}): NaCl, 115; KCl, 4; $CaCl_2$, 1.8; glucose, 11; Tris maleate 10, buffered to pH 7.4. Since the ganglia capsules were extremely hard and resisted cell impalements by microelectrodes, they were opened with forceps and the soma of Retzius neurones were exposed to the bathing fluid. Retzius neurones could be unequivocally identified by their characteristic size and position in the ganglion.

Morphology

The morphology of Retzius neurones and the possible locations of their contacts in the ganglion were studied by double intracellular staining, with Lucifer Yellow injected into one neurone and Texas Red into the other. Neither of these dyes crossed from one neurone to the other (see Fig. 1), as has previously been shown for Lucifer Yellow injections into Retzius neurones (Stewart, 1978). The dyes were pressure-injected into the soma of each neurone, and 30 min later the ganglia were fixed in 4% (w/v) paraformaldehyde in phosphate-buffered saline (PBS) for 2–12 h before being mounted in methyl salicylate and examined by confocal microscopy (Biorad, Hemel Hempstead, UK). Three-dimensional reconstructions of the branching patterns of single neurones or pairs of Retzius neurones were made from serial images taken every 0.5 μm. Reconstructions were carried out using Confocal Assistant 4.02 (Hemel Hempstead, UK) and Metamorph Imaging System 3.6 software (Universal Imaging, West Chester, PA, USA). Final images were produced using Adobe Photoshop 5.0 software (Adobe Systems, Mountain View, CA, USA).

Intracellular recordings

Microelectrodes for intracellular recordings were made with borosilicate glass of 1 mm exterior diameter and 0.75 mm internal diameter pulled in a P97 puller (Sutter Instruments). The microelectrodes had resistances of 18–25 MΩ when filled with 3 mol l^{-1} KCl. The presence of inhibitory synaptic potentials was explored using microelectrodes filled with 4 mol l^{-1} potassium acetate. Since there was no evidence of such activity and recordings were noisier than with KCl, the results presented here were obtained with electrodes filled with KCl.

Separate electrodes were used to inject current and to record voltage. This procedure was preferred over single-electrode current-clamp because, in many cases, fast and large biphasic current pulses were applied to produce artificial synaptic potentials and the speed of the switch mode limited the amount of current injected. A constraint of this technique is the decrease in somatic resistance caused by the penetration of the microelectrodes. Nevertheless, after a few minutes of recording, the membrane time constant and the amplitudes and kinetics of synaptic potentials were similar using one or two electrodes, and recordings could be maintained for several hours, suggesting a recovery of the input resistance. Intracellular recordings of up to 4 h showed no decrease in the resting potential, the somatic coupling ratio or the shape of the synaptic potentials.

Recordings were filtered using a costume-designed Bessel filter with a cut-off frequency of 600 Hz, which did not affect the rise time of the synaptic potentials. Data were acquired by an analog-to-digital board Digidata 1200 (Axon Instruments) at a sampling frequency of 20 kHz, using Axoscope software (Axon Instruments), and stored in a PC. Under these conditions, the recording noise was approximately 0.15 mV peak-to-peak, while the amplitudes of the smaller synaptic potentials were approximately 0.4 mV.

Data analysis

The rise times and the amplitudes of EPSPs were measured manually using Axoscope 8.0 and Clampfit 8.0 software (both from Axon Instruments). To express data, a convention was adopted in which V_1 was the voltage recording from the neurone into which current was injected or in which a synaptic potential was produced and V_2 was the voltage recording from the follower neurone. The coupling ratio either for steady-state voltages or for EPSPs was defined as the ratio of the amplitude of the follower voltage to that of the driving voltage, V_2/V_1. In the case of steady-state responses, these values were the voltage changes at the end of long current steps. In recordings of spontaneous activity, the nomenclature was used arbitrarily. Data are expressed as mean values ± the standard error of the mean (S.E.M.). Steady-state coupling ratios do not present variability, since only two or three measurements were made in every pair of neurones. The data presented are from the first test of the recording; one or two subsequent tests were made as controls at variable periods.

Results

Electrical coupling and potential contact sites between Retzius neurones

The characteristics of the steady-state electrical coupling between pairs of Retzius neurones, studied in 16 ganglia by simultaneous voltage recordings following current injection into either neurone, reproduced the earlier observations made in the leech *Hirudo medicinalis* (Hagiwara and Morita, 1962; Eckert, 1963). The resting potential of Retzius neurones was between −55 and −50 mV, which is close to the threshold for action potentials (−45 mV). Positive or negative currents

injected into the soma of either neurone spread equally well in both directions, suggesting no rectification. This was confirmed by the linear relationships between voltage and current amplitudes and between the amplitudes of the voltage changes in both somata (V_1 and V_2).

The possible sites of electrical contact between Retzius neurones were studied using three-dimensional confocal reconstruction of the arborizations of both neurones after one had been filled with Lucifer Yellow and the other with Texas Red. Presumably, the confocal overlap between the two neurones reflects possible areas of electrical coupling. Individual neurones were also filled with either dye to confirm that this would not spread to the adjacent neurone. Fig. 1A shows a three-dimensional reconstruction of one neurone injected with Lucifer Yellow. Although the soma of the other neurone can be seen, this was the result of intrinsic fluorescence and not of diffusion of dye from one neurone to the other. Similar images were obtained with both dyes, except that the intrinsic fluorescence was more intense in the fluorescein range. The shapes of both neurones were mirror images of each other and, in general, were very similar to the morphology of Retzius neurones in the leech *Hirudo medicinalis* (Lent, 1973; Smith et al., 1975; Mason and Leake, 1978). A primary process emerged from the cell body and produced four major secondary branches, one to the anterior ganglia, one to the posterior ganglia and the other two travelling to the periphery through the nerve roots. The primary process gave rise to multiple neurites that elongated within the neuropil.

In double-staining experiments, there was extensive overlap in the neuropilar arborizations of pairs of Retzius neurones. Since the somata produced severe optical interference, they were removed mechanically for confocal observations after aldehyde fixation. Fig. 1B shows one example in which the branches in yellow were filled with Lucifer Yellow and the branches in blue were filled with Texas Red. The white dots identify potential contact sites between the two neurones. The number of potential contact sites obtained from 18 different preparations ranged between 90 and 120, all established by fine neurites within the neuropil. Potential contact sites were absent from the somata or large processes of the neurones, suggesting that electrical coupling was restricted to the neuropil.

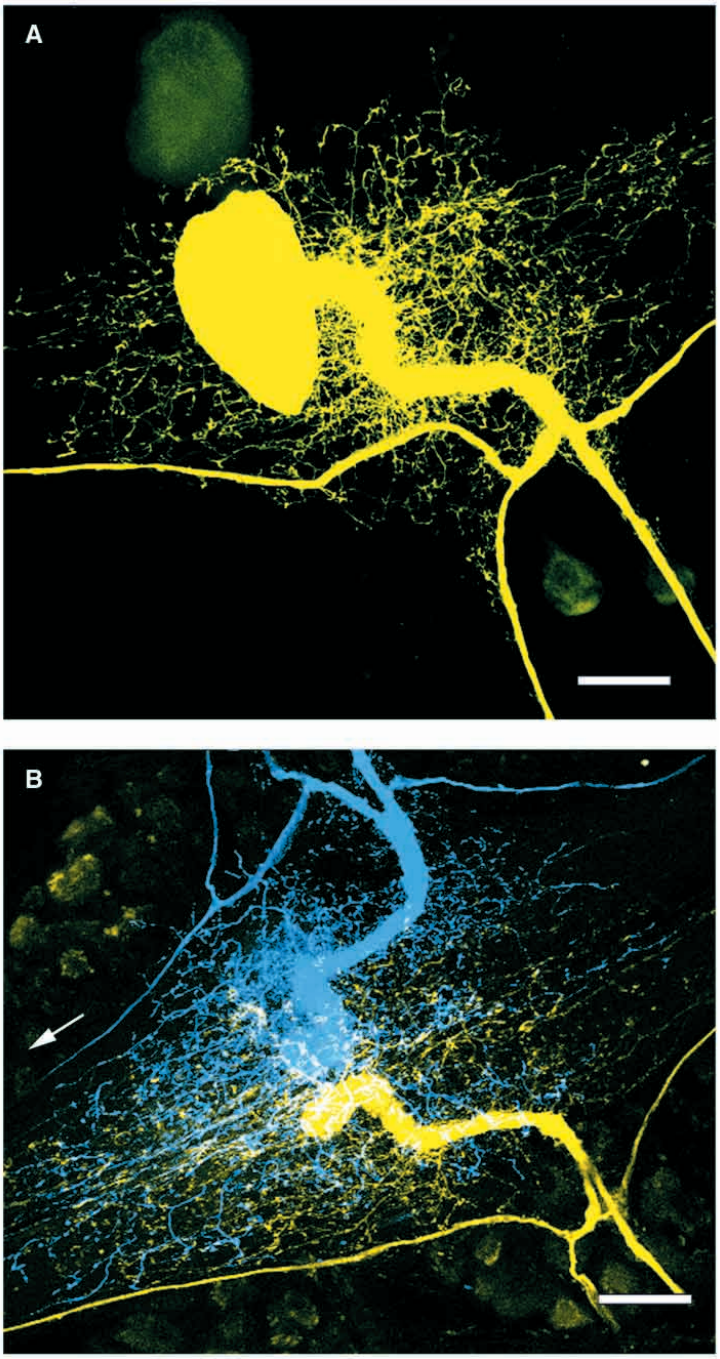

Fig. 1. Morphology and potential contact sites of Retzius neurones. (A) Three-dimensional reconstruction from serial confocal images of one Retzius neurone filled with Lucifer Yellow showing multiple fine neurites emerging from the primary process. The visualization of the somata of the contralateral neurone and of two small neurones in the lower right-hand corner resulted from autofluorescence. Anterior is to the left. (B) Three-dimensional confocal reconstruction of the dendritic arborization of a pair of Retzius neurones. The neurone coloured yellow was stained with Lucifer Yellow, while the blue neurone was injected with Texas Red. The somata were removed to avoid optical interference. Note the extensive dendritic overlap. The white dots are potential contact sites between the neurones. Autofluorescent somata of multiple neurones served to outline the ganglion. The arrow points to the anterior. Scale bar for both images, 30 μm.

Synaptic activity of Retzius neurones

Spontaneous pairs of synchronous EPSPs, appearing at an average frequency of $3.36\pm0.12\,s^{-1}$ (N=6), were recorded simultaneously from the soma of both Retzius neurones, suggesting a shared common input (Hawigara and Morita, 1962). Fig. 2A shows sequential series of simultaneous recordings from both somata. As can be seen, EPSPs could be abolished in a reversible manner when Ca^{2+} was substituted by Mg^{2+} in the external solution (Fig. 2B,C). Synaptic activity was always excitatory, and the characteristics of the EPSPs were similar when the recording electrodes were filled with potassium acetate or

with potassium chloride. In addition, synaptic events were not reversed when the resting potential of the neurones was held at voltage levels ranging from −80 to −40 mV by direct current injection into both somata (not shown), excluding the possibility of inhibitory synaptic potentials.

Excitatory postsynaptic potentials varied in their amplitude and kinetics from one event to the next. Fig. 3A shows a typical series of simultaneous recordings from a pair of Retzius neurones. As can be seen, the amplitudes of the synchronous EPSPs varied from one neurone to the other and from one event to the next. The simultaneous recordings at the top of Fig. 3A contain two pairs of synchronous EPSPs with inverse relationships in their amplitudes (marked with the asterisks). While the first EPSP in V_2 was approximately twice the amplitude of the corresponding EPSP in V_1, the following pair of EPSPs had the opposite relationship. In addition, there were synchronous events in which one EPSP was slower and smaller than that in the other neurone, as indicated by the arrows in Fig. 3A. An interpretation of these observations was that, when asynchronous transmission occurred, the fast EPSPs spread to the other neurone. The fluctuations in the amplitudes and kinetics of the synchronous EPSPs suggested that transmitter release onto each of the neurones was independent and variable, so that when it failed for one of the neurones an asynchronous EPSP was observed in dual recordings. Therefore, upon failures onto either neurone, the asynchronous EPSP could be recorded from both neurones.

In addition to the small EPSPs already described, approximately 15 % of the total number of events had much larger amplitudes. An example of this is shown in the bottom traces of Fig. 3A. Thus, when the distribution of the amplitudes of the EPSPs was plotted, two components were observed, as shown in Fig. 3B. One component had amplitudes ranging from 0.3 to 2.5 mV while the other had amplitudes ranging from 3.0 to 6.0 mV. While the small EPSPs had monotonic rising phases (Fig. 3C), the large EPSPs had complex rising phases, suggesting the summation of several small synaptic potentials (Fig. 3D). For this reason, only the population of low-amplitude events was used to test whether EPSPs spread from one neurone to another in the rest of this study.

Rise time distribution of EPSPs

The variations in the amplitude of the EPSPs and the possible sources for this variability (different quantal contents, different initiation sites and their spread through the gap junction) made it difficult to base our analysis on amplitude measurements. Instead, we used the rise times of EPSPs as the main source of information about their initiation sites and their spread to the contralateral neurone.

The rise time of EPSPs was variable, suggesting that they were produced at different electrotonic distances. Fig. 4A shows four EPSPs with different rise times and amplitudes (a–d), all recorded from the same neurone. The differences in the rise times could be an indication of the electrotonic distance at which they were produced. The rise times of EPSPs analysed in 22

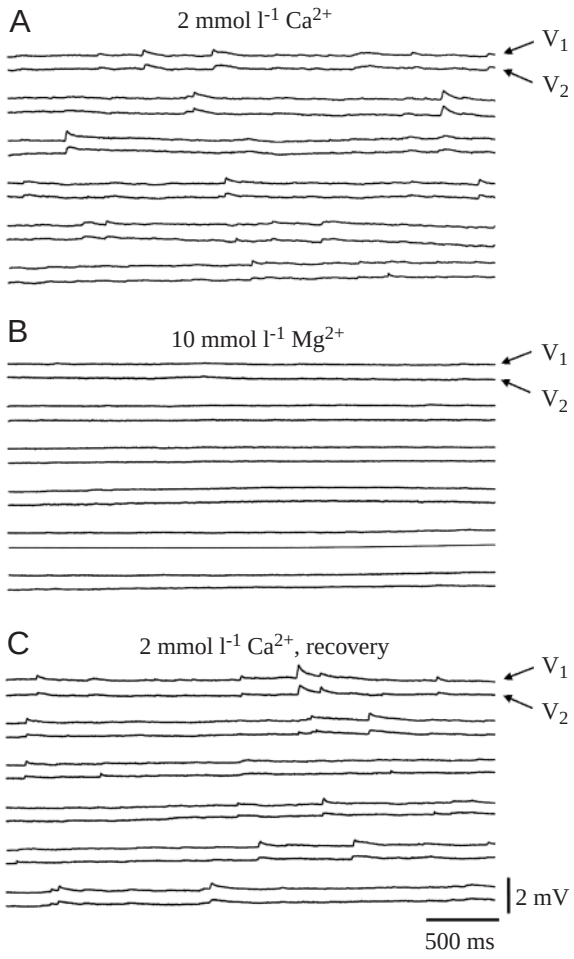

Fig. 2. Spontaneous synaptic activity in Retzius neurones. (A) Simultaneous somatic recordings of Retzius neurones in leech Ringer's solution showing spontaneous and synchronous excitatory postsynaptic potentials. V_1 is the recording from one of the neurones and V_2 is the recording from the other. Six consecutive series are shown. (B) Partial substitution of Ca^{2+} by Mg^{2+} in the Ringer's solution abolished the spontaneous activity in both neurones. (C) Synaptic activity was restored in normal Ringer's solution.

Retzius neurones ranged from 2 to 14 ms and were distributed in two populations when Gaussian functions were fitted to the data. One population had a major peak at 5.6±0.24 ms (N=11) and the other had a smaller peak at 9.6±0.33 ms containing 10–12 % of the events. An example of the rise time distribution of one neurone recorded in saline solution, is shown in Fig. 4B. The arrows indicate statistically significant peaks, the first at 5.97 ms and the second at 8.75 ms. When recordings were made with an external solution containing 1 mmol l^{-1} Ca^{2+} and 1 mmol l^{-1} Mg^{2+}, instead of the usual 1.8 mmol l^{-1} Ca^{2+}, the proportion of slow rising events increased to nearly 40 %, as shown in Fig. 4C. In this case, the fast rising peak was at 4.45 ms and the more slowly rising peak at 8.14 ms.

These results suggested that there were two major input domains to Retzius neurones. The fast-rising EPSPs were produced electrotonically closer to the recording site than those with the longer rise times. Considering that long-rise-time

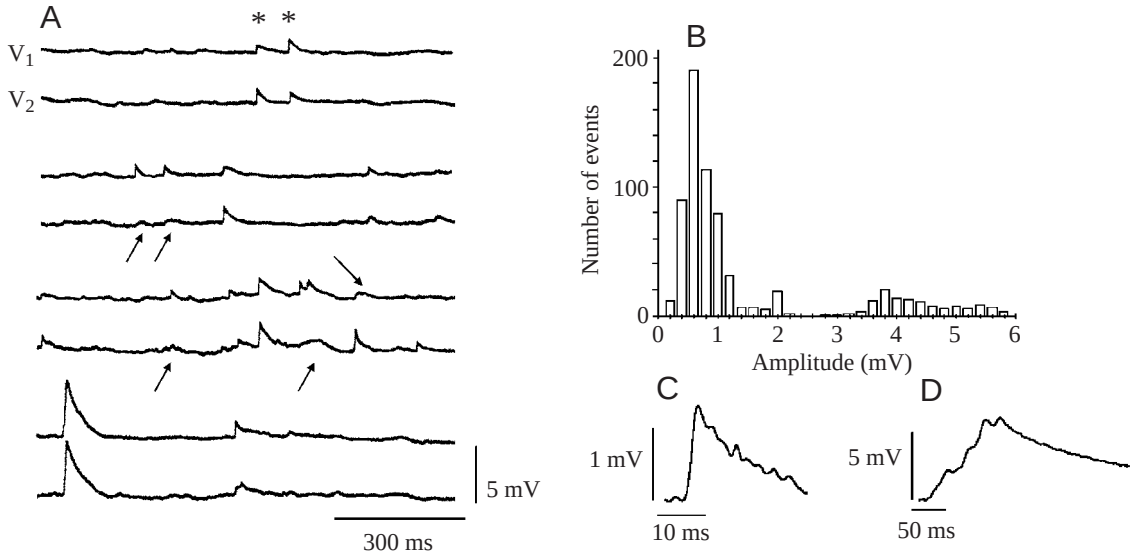

Fig. 3. Synaptic events in Retzius neurones. (A) Selected simultaneous recordings from a pair of Retzius neurones. V_1 is the recording from one of the neurones and V_2 is the recording from the other. The amplitudes of excitatory synaptic potentials (EPSPs) varied from one neurone to the other and from one event to the next in the same neurone (examples are marked by the asterisks). The arrows point to events that are slower and smaller than those in their contralateral partners, suggesting their spread from the other neurone. An example of a large EPSP can be seen at the bottom of the figure. (B) Amplitude distribution of EPSPs showing populations of small and large events (*N*=686). (C) The small events had monotonic rise times. (D) The large EPSPs had complex rising phases, suggesting the summation of several EPSPs. Note the scale differences between C and D.

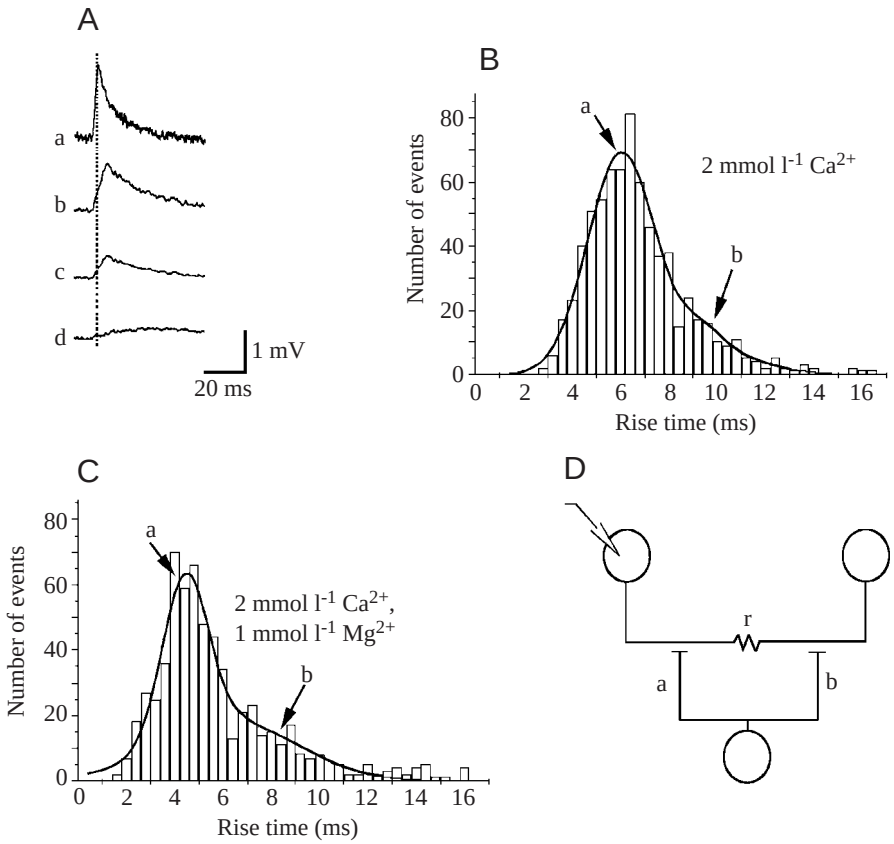

Fig. 4. Rise times of synaptic potentials. (A) Four excitatory postsynaptic potentials (EPSPs) with different rise times recorded from the same neurone. The dotted line passes through the peak of the fastest EPSP (a). The EPSPs shown in b and c had similar rise times but different amplitudes, suggesting either that they had been produced in the same site with different quantal contents or that the two EPSPs had been produced on different sides of the gap junction. The EPSP shown in d was smaller and slower, suggesting that it was produced electrotonically at a point more more distant from the soma being recorded. (B) Characteristic rise time distribution of one Retzius neurone recorded in normal saline solution. The distribution had two Gaussian components marked by the arrows. (C) The EPSP rise time distribution of a Retzius neurone recorded in the presence of 1 mmol l^{-1} Mg^{2+} in the external fluid. Again, two Gaussian peaks, which are marked by the arrows, were present. In this case, the peak at the long rise time was clearer. (D) Theoretical model showing two Retzius neurones with dendrites coupled by a resistance (r) and sharing a common presynaptic input. The lettering of the inputs corresponds to those in B and C and has as reference the recording electrode.

EPSPs could have arrived from the contralateral neurone, the clear separation between the two peaks suggested that most inputs were located between the gap junction and the soma of each Retzius neurone. A hypothetical circuit consisting of the pair of electrically coupled Retzius neurones, sharing a common synaptic input, is presented in Fig. 4D.

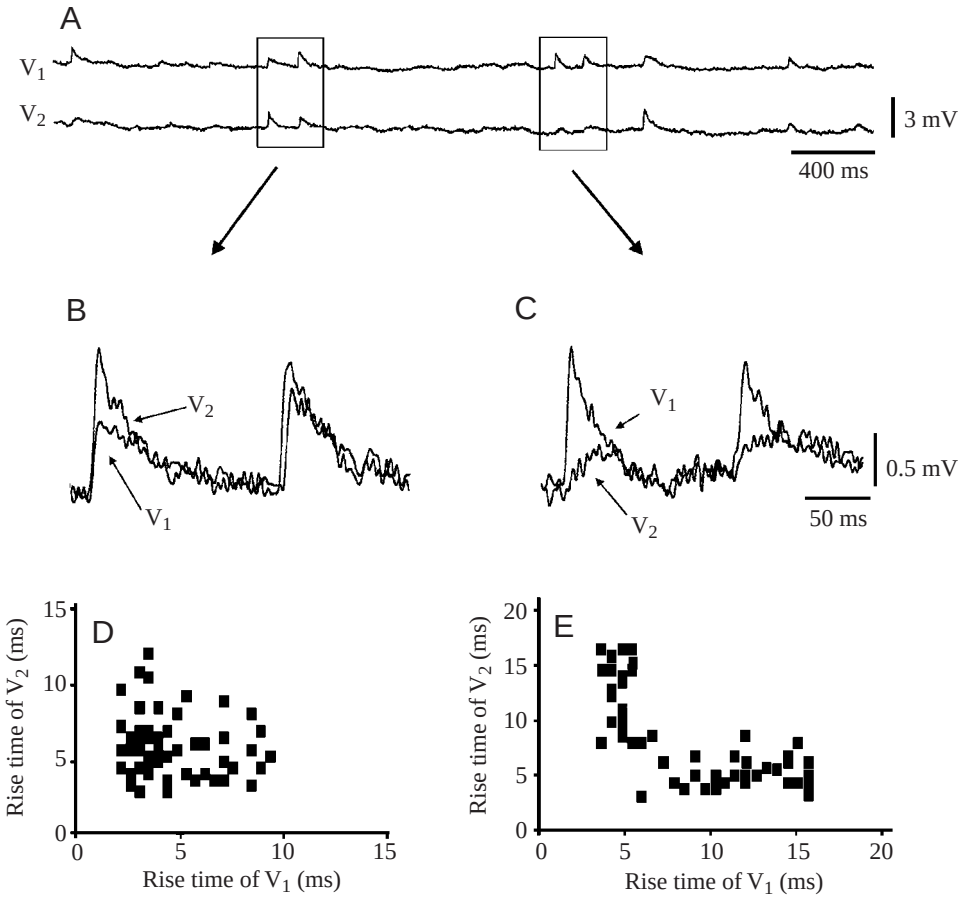

Fig. 5. Different relationships between pairs of synchronous excitatory postsynaptic potentials (EPSPs). V_1 is the recording from one of the neurones and V_2 is the recording from the other. (A) Simultaneous recordings from paired neurones showing pairs of synchronous EPSPs. (B) Amplification of two pairs of EPSPs from the first traces boxed in A, with different amplitudes but similar rise times. (C) In the second two pairs of synchronous EPSPs boxed in A, the amplitudes of EPSPs in V_2 were fractions of those in V_1 and the EPSPs had slower rise times, suggesting their propagation from V_1. (D) The relationship between the rise times of synchronous pairs of EPSPs in normal saline solution (*N*=60). (E) The relationship between the rise times of synchronous pairs of EPSPs in the presence of 1 mmol l^{-1} Mg^{2+} in the external solution in a different neurone (*N*=52). Fast times in V_1 clearly correlated with slow times in V_2 and *vice versa*.

Rise time relationships between synchronous EPSPs

To test whether the slowly rising EPSPs had their origin in the contralateral neurone, the kinetics of synchronous pairs of EPSPs were compared. The rise times of synchronous EPSPs showed two types of relationships. In 79 % of the synchronous pairs, both EPSPs had similar rise times. The two first pairs of synchronous EPSPs (boxed in Fig. 5A and amplified in Fig. 5B) varied in their amplitudes but had similar rise times. In the remaining 21 % of synchronous EPSP pairs, one EPSP had a fast rise time, which fell within the left side of the rise time distribution shown in Fig. 3B, and the other had a slow rise time. In addition, the amplitude of the slow EPSP was always a fraction of that of the fast one. Fig. 5C shows another segment of the recording shown in Fig. 5A. The amplitudes of the two slow EPSPs illustrated were 43 and 50 % of the amplitudes of their respective large EPSPs. A plot correlating the rise times of 60 pairs of subsequent EPSPs recorded in saline solution is presented in Fig. 5D. When 1 mmol l^{-1} Ca^{2+} was substituted for 1 mmol l^{-1} Mg^{2+} in the external solution, the percentage of pairs with one fast and one slow EPSP increased to 75.39 %. Under these conditions, there was a good correlation between the fast rise times in one neurone and the slow rise times in the other. One example is shown in Fig. 5E and represents 11 pairs of neurones.

Spread of artificial EPSPs

Indirect evidence that the slower and smaller EPSPs had arrived from the contralateral neurone came from the spread of artificial EPSPs produced by injection of brief biphasic current pulses into the soma of one neurone. Fig. 6A shows the protocol for current injection used to produce the artificial EPSPs. Note the scale values compared with the duration of the EPSPs. As shown in Fig. 6B, the shape of artificial EPSPs was similar to that of natural EPSPs recorded at the soma. In seven pairs of Retzius neurones, artificial synaptic potentials arrived at the contralateral soma attenuated and delayed. In the example shown in Fig. 6C, the coupling ratio of the artificial EPSP was 0.31±0.04 (*N*=10), smaller than the 0.42±0.01 (*N*=32) coupling ratio of pairs of naturally occurring EPSPs (Fig. 6D), and both were smaller than the 0.59 steady-state coupling ratio in these neurones, as expected for a passive spread of EPSPs through dendrites.

Steady-state and EPSP coupling ratios

To provide further information about the transynaptic flow of EPSPs, we tried to uncouple the electrical synapse pharmacologically. Unfortunately, heptanol, octanol and acetic acid, which uncouple gap junctions in other preparations, had no effect on this synapse at concentrations ranging from 0.1 to 20 mmol l^{-1}. Moreover, serotonin and octopamine, which modulate the electrical coupling in Retzius cells of the leech *Hirudo medicinalis* (Colombaioni and Brunelli, 1988), also failed in our hands. As an alternative, we compared the

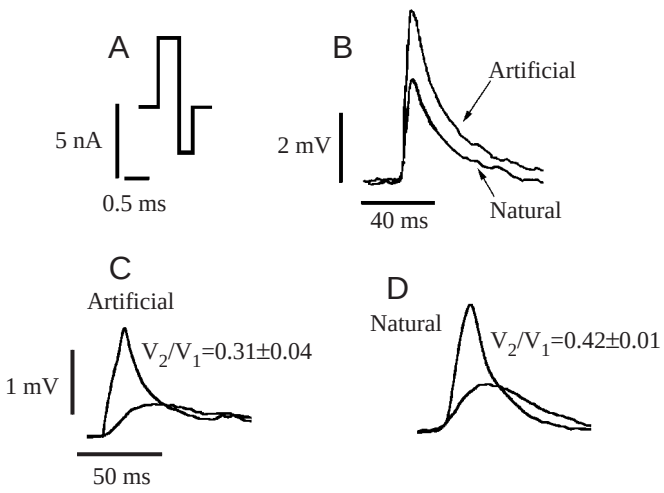

Fig. 6. Spread of artificial excitatory postsynaptic potentials (EPSPs) from one neurone to the other. (A) Current protocol used to produce artificial EPSPs in the soma of one of the neurones. (B) Artificial EPSP with a similar shape to natural EPSPs in the same neurone. (C) Artificial EPSPs arriving at the contralateral soma were smaller and had a slower rise time. The coupling ratio V_2/V_1, defined as the follower voltage (V_2) divided by the driving voltage (V_1), in these neurones was 0.31 (*N*=10). (D) The coupling ratio of natural EPSPs was 0.42 (*N*=32), greater than that of artificial EPSPs, as expected because of the different distances that each EPSP had to spread. Values given in the figure are means ± S.E.M.

coupling ratios of EPSP in pairs of neurones with different steady-state coupling ratios. In the 12 pairs tested, the rise time distributions and the range of amplitudes of EPSPs were very similar. We expect, therefore, that the variations in the steady-state coupling ratios were due to the coupling resistance and not to the dendritic membrane properties.

The results showed that, as expected, in these 12 pairs of Retzius neurones, the coupling ratios of EPSPs were always smaller than the steady-state coupling ratios. For example, in a pair of neurones that had a steady-state coupling ratio of 0.62 in the first 5 min of recording and at the end of the recording, the average coupling ratio of 34 EPSPs at the peak voltage values was 0.45±0.04. In the example shown in Fig. 7A, the steady-state coupling ratio was 0.31, while the coupling ratios of EPSPs were between 0.20 and 0.26 (Fig. 7B). Note that, despite the low coupling ratio, the amplitudes and shapes of EPSPs corresponded to those described above. Mean coupling ratios of 35 EPSPs in 12 different pairs of neurones with coupling ratios from 0.31 to 0.72 are plotted in Fig. 7C. A line of slope 1 is drawn to highlight the fact that the coupling ratios of EPSPs were, in all cases, smaller than those of steady-state pulses.

Discussion

We have shown that electrical coupling between Retzius neurones serves as a bridge for EPSP spread from one neurone to another. The presence of synchronous EPSPs in pairs of Retzius neurones suggests a common and as yet unidentified synaptic input (or inputs) with spontaneous activity. Similar results were obtained in Retzius neurones (Hagiwara and Morita, 1962) and touch-sensitive neurones of the leech *Hirudo medicinalis* (Baylor and Nicholls, 1969). The amplitudes of synchronous EPSPs varied independently from one neurone to the other and from one event to another, suggesting probabilistic release of transmitter from presynaptic endings. These variations also suggest that asynchronous transmission may result from transmission failures onto either of the neurones. This is supported by the increase in the proportion of asynchronies in the presence of Mg^{2+} in the recording solution.

The rise time distribution of EPSPs recorded from individual neurones suggests two major input domains. Excitatory postsynaptic potentials with short rise times could, therefore, be produced by inputs between the gap junction and the

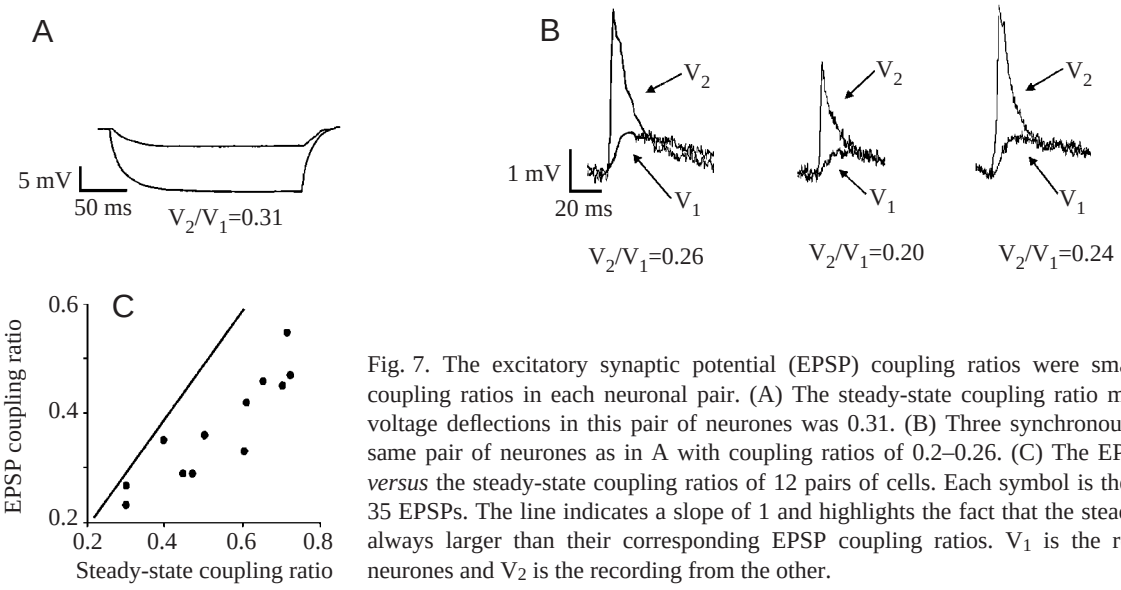

Fig. 7. The excitatory synaptic potential (EPSP) coupling ratios were smaller than the steady-state coupling ratios in each neuronal pair. (A) The steady-state coupling ratio measured by the end of the voltage deflections in this pair of neurones was 0.31. (B) Three synchronous pairs of EPSPs from the same pair of neurones as in A with coupling ratios of 0.2–0.26. (C) The EPSP coupling ratios plotted *versus* the steady-state coupling ratios of 12 pairs of cells. Each symbol is the average coupling ratio of 35 EPSPs. The line indicates a slope of 1 and highlights the fact that the steady-state coupling ratios are always larger than their corresponding EPSP coupling ratios. V_1 is the recording from one of the neurones and V_2 is the recording from the other.

recording electrode. The equivalent input to the other neurone would produce the long-rise-time EPSPs (see Fig. 4). The overlapping zones of the rise time distribution may reflect inputs closer to the gap junctions. Since the kinetics of these EPSPs would be very similar in both neurones, without pharmacological uncoupling it is extremely difficult to determine on which side of the gap junction they were produced.

Electrical properties and coupling resistance of Retzius neurones

Fundamental factors for the integrative processes are the electrical properties of the neuronal membranes. Contact sites between Retzius neurones in other species are supposed to be established by proximal dendrites rising from the primary segmental axon of the neurones (Lent, 1973; Smith et al., 1975; Mason and Leake, 1978). Our morphological analysis suggests that EPSPs have to spread for distances of between 100 and 200 μm to arrive at the soma. Since action potentials are initiated in the primary process of these neurones (F. F. De Miguel, unpublished observation), the spread of EPSPs to the soma predicts a large space constant. However, the fact that the coupling ratio of natural or artificial EPSPs was smaller than the steady-state coupling ratio indicates that membrane filtering contributes to the EPSP coupling ratio.

Our evidence also supports a contribution of the coupling resistance to the somatic coupling ratio. First, since EPSPs are produced relatively close to the gap junction, their decay to both somata should be similar and, therefore, a large proportion of their coupling ratio must be due to the coupling resistance. Second, the coupling ratios of EPSPs and steady-state pulses of different pairs of neurones with similar electrophysiological properties suggest that these differences arise from the coupling resistance value. This is in agreement with previous evidence showing the combined contribution of cable properties and coupling resistance to the somatic coupling of Retzius neurones (Yang and Chapman, 1983).

Expected effects of electrical coupling to integration

An expected effect of the coupling resistance value is that, when it is high, the dendritic impedance will increase, tending to the formation of a ‘sealed end’ (Rall, 1958), improving current spread towards the soma of the same neurone. In these conditions, each Retzius neurone would integrate almost independently from the other. In contrast, when the coupling resistance value is low, the two dendrites would tend to be in electrical continuity, thus resembling a semi-infinite cable and leading to reduced dendritic impedance but improved trans-junctional current spread. The EPSPs arriving from the other neurone (alien EPSPs) would, therefore, be more influential for integration. A benefit of a low coupling resistance would be that the firing frequency of the neurone would increase as a result of summation of local with alien EPSPs.

An expected consequence of the synchrony of most EPSPs in Retzius neurones is that, if the inputs were distant from each other, part of the current of one EPSP would flow towards the contralateral soma, adding mostly to the decay phase of the other EPSP. This would reduce the membrane filtering effect of the EPSPs, improving their conduction. In contrast, if synchronous EPSPs were produced on either side of the gap junction, the summation would affect the amplitudes and not the wave shape. Therefore, with short distances between the initiation sites of EPSPs, summation of EPSPs would affect the gain, whereas an increase in the distance between the inputs would reduce the effect on the amplitude and would affect the decay phase. Experiments combining artificial synaptic potentials with computational modelling should help to solve this problem.

The different electrotonic distances at which EPSPs are produced and their flow through gap junctions may explain why the amplitude distribution of the population of EPSPs does not reflect a quantal phenomenon (Fig. 3B). The increasing evidence of electrical coupling between mammalian neurones makes it interesting to explore whether, in some of the quantal analysis mismatches in central vertebrate neurones, electrical coupling has obscured the interpretation of results (for a review, see Faber et al., 1998).

Possible general significance

An increasing amount of evidence from electrophysiological experiments and from the expression patterns of gap junction proteins indicates that a large proportion of central neurones in embryonic and adult nervous systems of vertebrates, including mammals, display electrical coupling (Bruzzone et al., 1996; Nadarajah et al., 1996; for a review, see Dermietzel and Spray, 1993). Among the functions of electrical synapses, the mediation of fast behavioural responses in crustaceans (Furshpan and Potter, 1959) and fishes (Lin and Faber, 1988) and also the synchronization of groups of neurones in vertebrates, including mammals (Christie et al., 1989; Valiante et al., 1995; Ishimatsu and Williams, 1996; Mann-Metzer and Yarom, 1999; Galarreta and Hestrin, 1999; Gibson et al., 1999), have been demonstrated. Other possible functions, including transmitter coupling (Vaney et al., 1998) and second-messenger coupling (Dermietzel and Spray, 1993), have also been proposed. Even though electrical coupling in invertebrates is mediated by a different set of proteins (Bacon et al., 1998), the fact that some functions of electrical coupling are conserved between invertebrates and vertebrates makes it very likely that EPSP spread may also be conserved in higher animals.

We are greatly indebted to Mr Bruno Mendez for his invaluable technical assistance in our experiments. We also wish to acknowledge the Computing and Microscopy Units at our Institute for their continuous support during this project. We thank Dr Lidia Szczupak for her critical discussion on the data. E.G.P. was supported by CONACYT and DGEP fellowships. M.V.C. and E.G.P. received complementary fellowships from a Human Frontiers Science Program grant (RG-162/98) to F.F.M. Human Frontiers Science Program (RG-162/98), CONACYT (1285-N9204) and PAPIIT (IN-207593) grants to F.F.M. have supported this project.

References

Abbott, L. F., Marder, E. and Hooper, S. L. (1991). Oscillating networks: control of burst duration by electrically coupled neurons. *Neural Comput.* **3**, 487–497.

Andersen, P., Holmquist, B. and Voorhoeve, P. E. (1966). Excitatory synapses on hippocampal apical dendrites activated by entorhinal stimulation. *Acta Physiol. Scand.* **66**, 461–472.

Auerbach, A. A. and Bennett, M. V. L. (1969). A rectifying electrotonic synapse in the central nervous system of a vertebrate. *J. Gen. Physiol.* **53**, 211–237.

Bacon, J. P., Phelan, P., Davies, J., Stebbings, L. and Toodmand, M. G. (1998). Innexins: a family of invertebrate gap-junctions proteins. *Trends Genet.* **14**, 477–483.

Baker, R. and Llinás, R. (1971). Electrotonic coupling between neurones in the rat mesencephalic nucleus. *J. Physiol., Lond.* **212**, 45–63.

Baylor, D. A. and Nicholls J. G. (1969). Chemical and electrical synaptic connections between cutaneous mechanoreceptor neurons in the central nervous system of the leech. *J. Physiol., Lond.* **203**, 591–609.

Bennett, M. V. L., Aljure, E., Nakajima, Y. and Pappas, G. D. (1963). Electrotonic junctions between teleost spinal neurons: electrophysiology and ultrastructure. *Science* **141**, 262–263.

Bruzzone, R., White, T. W. and Paul, D. L. (1996). Connections with connexins: the molecular basis of direct intercellular signaling. *Eur. J. Biochem.* **238**, 1–27.

Christie, M. J., Williams, J. T. and North, R. A. (1989). Electrical coupling synchronizes subthreshold activity in locus coeruleus neurons *in vitro* from neonatal rats. *J. Neurosci.* **9**, 3584–3589.

Colombaioni, L. and Brunelli M. (1988). Neurotransmitter-induced modulation of an electrotonic synapse in the CNS of *Hirudo medicinalis*. *Exp. Biol.* **47**, 139–144.

Coombs, S. J., Curtis, D. R. and Eccles, J. C. (1957). The interpretation of spike potentials of motoneurones. *J. Physiol., Lond.* **139**, 198–231.

Deisz, R. A., Fortin, G. and Zieglgaensberger, W. (1991). Voltage dependence of excitatory synaptic potentials in rat neocortical neurons. *J. Neurophysiol.* **65**, 371–382.

Dermietzel, R. and Spray, D. C. (1993). Gap junctions in the brain: where, what type, how many and why? *Trends Neurosci.* **16**, 186–192.

Eckert, R. (1963). Electrical interaction of paired ganglion cells in the leech. *J. Gen. Physiol.* **46**, 573–587.

Faber, D., Korn, H., Redman, S. J., Thompson, S. C. and Altman, J. (1998). *Central Synapses, Quantal Mechanisms and Plasticity*. Human Frontiers Science Program Workshop Reports. Strasbourg: The Human Frontiers Science Program.

Fatt, P. (1957). Sequence of events in synaptic activation of a motoneurone. *J. Neurophysiol.* **20**, 61–80.

Furshpan, E. J. and Potter, D. D. (1959). Transmission at the giant motor synapses of the crayfish. *J. Physiol., Lond.* **145**, 289–325.

Galarreta, M. and Hestrin, S. (1999). A network of fast-spiking cells in the neocortex connected by electrical synapses. *Nature* **402**, 72–75.

Gibson, J. R., Beierlein, M. and Connors, B. W. (1999). Two networks of electrically coupled inhibitory neurons in neocortex. *Nature* **402**, 75–79.

Gillessen, T. and Alzheimer, C. (1997). Amplification of EPSPs by low $Ni^{(2+)}$ and amiloride-sensitive $Ca^{(2+)}$ channels in apical dendrites of rat CA1 pyramidal neurons. *J. Neurophysiol.* **77**, 1639–1643.

Haag, J. and Borst, A. (1996). Amplification of high frequency synaptic inputs by active dendritic membrane processes. *Nature* **379**, 639–641.

Hagiwara, S. and Morita, H. (1962). Electrotonic transmission between two nerve cells in the leech ganglion. *J. Neurophysiol.* **25**, 721–731.

Hatton, G. I. and Yang, Q. Z. (1994). Incidence of neuronal coupling in supraoptic nuclei of virgin and lactating rats: estimation by neurobiotin and Lucifer Yellow. *Brain Res.* **650**, 63–69.

Henderson, L. (1983). The role of 5-hydroxytryptamine as a transmitter between identified leech neurons in culture. *J. Physiol., Lond.* **339**, 311–326.

Hirsch, J. A. and Gilbert, C. D. (1991). Synaptic physiology of horizontal connections in the cat's visual cortex. *J. Neurosci.* **11**, 1800–1809.

Ishimatsu, M. and Williams, J. T. (1996). Synchronous activity in locus coeruleus results from dendritic interactions in pericoerulear regions. *J. Neurosci.* **16**, 5196–5204.

Korn, H., Sotelo, C. and Crepel, F. (1973). Electronic coupling between neurons in the rat lateral vestibular nucleus. *Exp. Brain Res.* **16**, 255–275.

Kristan, W. B. (1982). Sensory and motor neurons responsible for the local bending response in leeches. *J. Exp. Biol.* **96**, 161–180.

Lent, C. M. (1973). Retzius cells from segmental ganglia of four species of leeches: comparative neuronal geometry. *Comp. Biochem. Physiol.* **44A**, 35–40.

Lin, J. W. and Faber, D. (1988). Synaptic transmission mediated by single club endings on the goldfish Mauthner cell. I. Characteristics of electrotonic and chemical postsynaptic potentials. *J. Neurosci.* **8**, 1302–1312.

Lipowsky, R., Gillessen, T. and Alzheimer, C. (1996). Dendritic Na^+ channels amplify EPSPs in hippocampal CA1 pyramidal cells. *J. Neurophysiol.* **4**, 2181–2191.

Llinás, R., Baker, R. and Sotelo, C. (1974). Electrotonic coupling between neurons in cat inferior olive. *J. Neurophysiol.* **37**, 560–571.

Llinás, R. and Hess, R. (1976). Tetrodotoxin-resistant dendritic spikes in avian Purkinje cells. *Soc. Neurosci. Abstr.* **2**, 112.

Llinás, R. and Nicholson, C. (1971). Electroresponsive properties of dendrites and somata in alligator Purkinje cells. *J. Neurophysiol.* **34**, 532–551.

Llinás, R. and Sugimori, M. (1980). Electrophysiological properties of *in vitro* Purkinje cells in mammalian cerebellar slices. *J. Physiol., Lond.* **305**, 197–213.

Lockery, S. R. and Kristan, W. B. (1990). Distributed processing of sensory information in the leech. II. Identification of interneurones contributing to the local bending reflex. *J. Neurosci.* **10**, 1816–1829.

Mann-Metzer, P. and Yarom, Y. (1999). Electrotonic coupling interacts with intrinsic properties to generate synchronized activity in cerebellar networks of inhibitory interneurons. *J. Neurosci.* **19**, 3298–3306.

Marder, E. and Eisen, J. S. (1984). Electrically coupled pacemaker neurons respond differently to the same physiological inputs and neurotransmitters. *J. Neurophysiol.* **51**, 1362–1373.

Margulis, M. and Tang, C. M. (1998). Temporal integration can readily switch between sublinear and supralinear summation. *J. Neurophysiol.* **79**, 2809–2813.

Mason, A. and Leake, L. D. (1978). Morphology of leech Retzius cells demonstrated by intracellular injection of horseradish peroxidase. *Comp. Biochem. Physiol.* **61A**, 213–216.

McMahon, D. G. (1994). Modulation of synaptic transmission in zebrafish retinal horizontal cells. *J. Neurosci.* **14**, 1722–1734.

Nadarajah, B., Thomaidou, D., Evans, W. H. and Parnavelas, P. G. (1996). Gap junctions in the adult cerebral cortex: regional differences in their distribution and cellular expression of connexins. *J. Comp. Neurol.* **376**, 326–342.

Nicholls, J., Martin, A. R. and Wallace, B. G. (1992). *From Neuron to Brain*. Sunderland, MA: Sinauer.

Nicholls, J. G. and Purves, D. (1972). A comparison of chemical and electrical synaptic transmission between single sensory cells and a motoneurone in the central nervous system of the leech. *J. Physiol., Lond.* **225**, 637–656.

Nusbaum, M. P., Friesen, W. O., Kristan, B. W. and Pierce, R. A. (1987) Neural mechanisms generating the leech swimming rhythm. *J. Comp. Physiol.* **161A**, 355–366.

Nusbaum, M. P. and Kristan, B. W. (1986). Swim initiation in the leech by serotonin-containing interneurones, cells 21 and 61. *J. Exp. Biol.* **122**, 277–302.

Payton, B. (1981). The structure of the leech nervous system. In *Neurobiology of the Leech* (ed. K .J. Muller, J. G. Nicholls and G. S. Stent), pp. 35–50. New York: Cold Spring Harbor Laboratory.

Rall, W. (1958). Mathematical solutions for passive electrotonic spread between a neuron soma and its dendrites. *Fedn. Proc.* **17**, 127.

Sahley, C. L. (1995). What we have learned from the study of learning in the leech. *J. Neurobiol.* **27**, 434–445.

Schmalbruch, H. and Jahnsen, H. (1981). Gap junctions on CA3 pyramidal cells of guinea pig hippocampus shown by freeze–fracture. *Brain Res.* **217**, 175–178.

Schwindt, P. C. and Crill, W. E. (1995). Amplification of synaptic current by persistent sodium conductance in an apical dendrite of neocortical neurons. *J. Neurophysiol.* **74**, 2220–2224.

Seamans, J. K., Gorelova, N. A. and Yang, C. R. (1997). Contributions of voltage-gated Ca^{2+} channels in the proximal versus distal dendrites to synaptic integration in prefrontal cortical neurons. *J. Neurosci.* **17**, 5936–5948.

Smith, P. A., Sunderland, L. D., Leake, L. D. and Walker, R. J. (1975). Cobalt staining and electrophysiological studies of Retzius cells in the leech *Hirudo medicinalis*. *Comp. Biochem. Physiol.* **51A**, 665–661.

Spencer, W. A. and Kandel, E. R. (1961). Electrophysiology of hippocampal neurons. IV. Fast prepotentials. *J. Neurophysiol.* **24**, 272–285.

Stewart, W. W. (1978). Intracellular marking of neurons with a highly fluorescent naphthalimide dye. *Cell* **14**, 741–759.

Stuart, G. and Sakmann, B. (1995). Amplification of EPSPs by axosomatic sodium channels in neocortical pyramidal neurons. *Neuron* **15**, 1065–1076.

Szczupak, L. and Kristan, W. B. (1995). Widespread mechanosensory activation of the serotonergic system of the medicinal leech. *J. Neurophysiol.* **74**, 2614–2624.

Valiante, T. A., Pérez-Velázquez, J. L., Jahromi, S. S. and Carlen, P. L. (1995). Coupling potentials in CA1 neurons during calcium-free-induced field burst activity *J. Neurosci.* **15**, 6946–6956.

Vaney, D. T., Nelson, J. C. and Pow, D. V. (1998). Neurotransmitter coupling through gap junctions in the retina. *J. Neurosci.* **18**, 10594–10602.

Wessel, R., Kristan, W. B. and Kleinfeld, D. (1999). Supralinear summation of synaptic inputs by an invertebrate neuron: dendritic gain is mediated by an 'inward rectifier' K^+ current. *J. Neurosci.* **19**, 5875–5888.

Willard, A. L. (1981). Effects of serotonin on the generation of the motor program for swimming by the medicinal leech. *J. Neurosci.* **1**, 936–944.

Wolszon, L. R., Passani, M. B., Macagno, E. R. (1995). Interactions during critical period inhibit bilateral projections in embryonic neurons. *J. Neurosci.* **15**, 1506–1515.

Yang, J. and Chapman, K. M. (1983). Frequency domain analysis of electrotonic coupling between leech Retzius cells. *Biophys. J.* **44**, 91–99.

Yuste, R. and Tank, D. W. (1996). Dendritic integration in mammalian neurons, a century after Cajal. *Neuron* **16**, 701–716.